Journal of Ovonic Research Vol. 10, No. 6, November - December 2014, p. 257 - 263

TETRA BLENDED BASED HYBRID BULK HETEROJUNCTION SOLAR CELLS

M. IKRAM[a,b], N. A. NIAZ[c*], N.R. KHALID[c] , M.Ramzan[c], M. IMRAN[d], S. ALI[b]
[a]*Department of Materials Science and Engineering, University of Delaware, USA 19716*
[b]*Solar Application Lab, Department of Physics, G. C. University Lahore, Punjab 54000, Pakistan*
[c]*Department of Physics, Bahauddin Zakariya University, 68000, Multan*
[d]*Technical Institute of Physics and Chemistry, Chinese Academy of Sciences, 29 Zhongguancun East Road, Haidian District, Beijing 100190, China*
.

In this paper, we investigated the effects of mixing TiO_2 and ZnO nanoparticles in the photoactive layer of poly (3-hexylthiophene) (P3HT) and [6,6]-phenyl C61-butyric acid methyl ester (PCBM) solar cells. Different weight ratios of TiO_2, ZnO nanoparticles and PCBM were mixed, keeping the constant ratio of P3HT to form blend for deposition of active layer using xylene as a solvent. The mixing of both nanoparticles in the active layer of P3HT:PCBM increased the power conversion efficiency (PCE) of the devices. The optical absorption was enhanced in the visible region with the addition of TiO_2 and ZnO nanoparticles in the active layer. The roughness of the active layer was increased with increasing amount of nanoparticles in the active layer blend. The metal oxides nanoparticles were found to agglomerate as their concentration increases than PCBM in the active layer and completely agglomerate in the absence of PCBM.

(Received October 1, 2014; Accepted December 5, 2014)

Keywords: Blend; Active layer; P3HT, PCBM; Solvent; $TiO_{2;}$ ZnO nanoparticles

1. Introduction

Organic solar cells (OSCs) are a smart technology because of their prospect ease fabrication, low cost, lightweight, readily available, colorful and portable [1–4]. In spite of having low efficiency and short lifetimes, the latest cost effective reports suggest that OSCs could become economical with other solar cell if modules with PCE of 5% and five years stability could be manufactured. One of the most promising techniques to enhance the PCE of the device is to build up interpenetrating network of electron donor and acceptor components in the photoactive layer of the solar cells.

More recently, various hybrid organic-inorganic nanocrystals solar cells have been reported using different organic semiconductors P3OT, P3HT, MEH-PPV [5–11] and inorganic nanocrystals CdS, CdSe, CdTe, ZnO, SnO_2, TiO_2, PbS, and PbSe [12–20]. It was reported that incorporation of metal oxides in the active layer enhance the stability composed of P3HT, but also improved the charge transfer and thus PCE of hybrid solar cells [21,22]. Organic semiconductor have high light absorption coefficient compared to Si and inorganic nanoparticles have high carrier mobilities and higher absorption coefficient than PCBM generally used in organic solar cells [23].

In this study, ZnO and TiO_2 nanoparticles were mixed in the blend of organic materials to fabricate tetra blended hybrid bulk heterojunction solar cells. Efforts have been made to replace PCBM in polymer solar cells; in addition to being less expensive than PCBM the inorganic

---

[*] Corresponding author: niazpk80@bzu.edu.pk

materials have energy levels that have capability to align with the electron donor (P3HT). The mixing of both metal oxides in the active layer of P3HT:PCBM solar cells, it can enhance the charge mobility and shrink the cost of the devices. Therefore, we fabricated devices with a P3HT:PCBM:ZnO:TiO_2 blend.

2. Experimental details

ZnO nanoparticles (≤100 nm) were purchased from Sigma-Aldrich and titanium dioxide nanoparticles (8-10 nm) were synthesized based on technique [24]. Regio-regular P3HT was purchased from Rieke Metals. PCBM (99 % purity) was purchased from Nano-C USA. The hole transport layer poly(3,4 polyethylene dioxythiophene polystyrenesulfonate) PEDOT:PSS was received from Heraeus Material Technology LLC, USA. ITO coated glass substrates were purchased from Delta Technologies USA.

Indium tin oxide (ITO) coated on a glass substrates were cleaned in detergent, deionized water, isopropanol and acetones for 5 minutes each. Substrates were dried in nitrogen pressure and placed into a UV-O_3 cleaner for 20 minutes. The conducting polymer poly (3,4-ethylenedioxythiophene):poly(styrene-sulfonate) (PEDOT:PSS) was spin coated using 3000 rpm for 60 seconds and used as anode buffer material for smoothing the ITO surface, enhancing the adhesion to the upper light absorbing layer, and improving the device stability by hindering oxygen and indium diffusion through the anode. The blend of P3HT:PCBM:ZnO:TiO_2 of different weight ratios (1:0.7:0 A, 1:0.55:0.075:0.075 B, 1:0.35:0.175:0.175 C, 1:0.15:0.275:0.275 D and 1:0:0.35:0.35 E) dissolved in 1ml xylene (X) solvent after stirring 12 hrs at 40^0C was spuned on the top of PEDOT:PSS layer. Finally, a top metal electrode of LiF/Al was vacuum deposited onto the photoactive layer. The top contact area of 0.4 cm^2 was maintained for all devices. We fabricated all the devices twice time and found very small change in PCE of the devices.

3. Results and Discussion

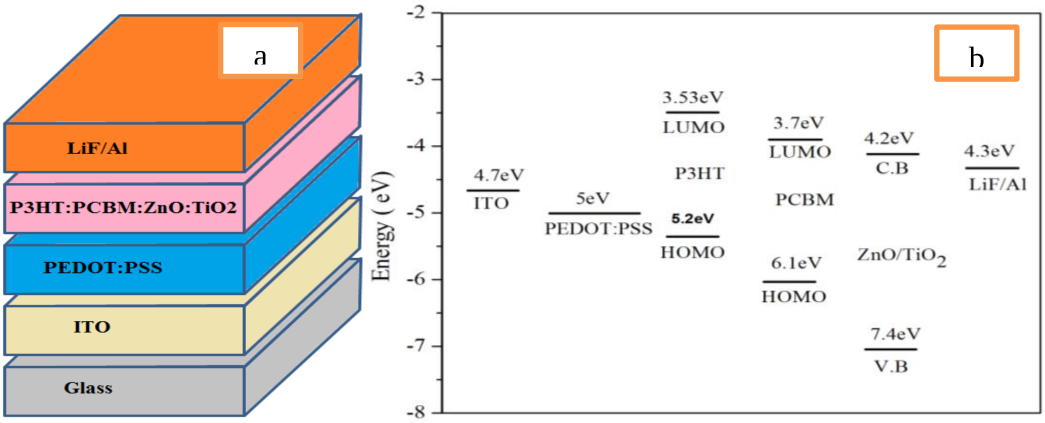

Fig. 1: Schematic of hybrid BHJ solar cell (a) and energy level diagram (b)

Fig. 1a depicts the architecture of normal hybrid BHJ solar cell with the photoactive layer composed of P3HT, PCBM and ZnO:TiO_2 nanoparticles. The energy level diagram of the layers involved for the ZnO:TiO_2 conjugated hybrid solar cells [25] is shown in Fig. 1b. Photogenerated excitons are generated at the interfaces of donor (P3HT) and acceptor (PCBM). In this case the generated holes transfer towards the ITO anode after passing through buffer layer (PEDOT:PSS) and electrons are transported to the LiF/Al cathode. Electrons cannot flow towards ITO electrode due to PEDOT:PSS. The mixing of ZnO and TiO_2 nanoparticles in the active layer favor transport electrons towards top contact (Al) due to their lower conduction energy level and higher electron mobility in the hybrid active layer.

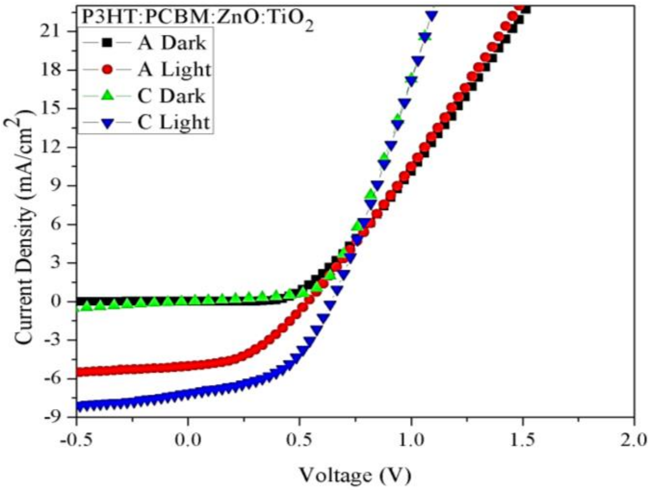

Fig. 2: J-V characteristics of various ratios of P3HT:PCBM:ZnO:TiO$_2$.

The current density vs voltage (J-V) curves obtained under dark and light conditions using a calibrated AM 1.5 G solar simulator at 100 mW/cm^2 are shown in Figure 2. Different weight ratios of the blends were used in the active layer and results are summerized in Table 1.

Table 1: Device parameters obtained from J-V curves in Fig. 2

Devices	V_{oc} (V)	J_{sc} (mA/cm^2)	FF (%)	R_{sh} (Ω-cm^2)	R_s (Ω-cm^2)	PCE (%)
A	0.54	5.03	41.7	676	39.2	1.13±0.1
B	0.64	5.78	53.7	1064	15.6	1.98±0.2
C	0.64	7.16	48.4	362	16.8	2.22±0.03
D	0.64	5.53	44.4	696	22.0	1.55±0.2
E	0.28	0.01	34.1	26240	50.4	0.001±0.0

As we incorporated ZnO:TiO$_2$ nanoparticles to the active layer of the devices, better performance in nearly every parameters is found, namely Voc, Rs and Jsc. This trend broke down with very higher concentration of metal oxides without PCBM in the binary active layer blend. This is probably due to large aggregations of nanoparticles preventing charge separation and reducing the short circuit current to zero. The table indicates that mixing various ratios of ZnO:TiO$_2$ nanoparticles in the active layer of the devices, while maintaining the amount of acceptor material, increased efficiency from 1.13± 0.1 % to 2.22± 0.03 %. The increase in efficiency mostly originates from a drop in series resistance (Rs) with the incorporation of optimum amount of metal oxides nanoparticles in the active layer, evident from the high Jsc when similar values of voltages are applied. The table shows that Rs decreased from 39.2 **Ω**-cm^2 to 22.0 **Ω**-cm^2 with incorporation of metal oxides, in the presence of PCBM in the active layer. The decrease in Rs is manifested to decrease in bulk resistivity with the addition of ZnO:TiO$_2$ as the addition develops perculation network of the active layer [26]. The increase in Rsh is due to suppression of leakage current attributed to nanoparticles network [13,27]. The observed increase in Rsh and decrease in Rs, reduced the leakage current and found significant increase in FF and Voc of the devices with increasing amount of nanoparticles in the active layer [28,29]. The increase observed in J_{sc} and FF is attributed to percolation network of nanoparticles that facilitates the electron transport in the photoactive layer and an electric field is formed between heterojunction of organic material and nanoparticles [25,30]. The Voc remained constant in the devices, untill whole PCBM was replaced by ZnO:TiO_2, when the Voc is droped to 0.28 V. This decrease in Voc is due to the BHJ structure breaking down from extensive aggregations of the metal oxides in the binary blend and can be seen in device E (Table 1).

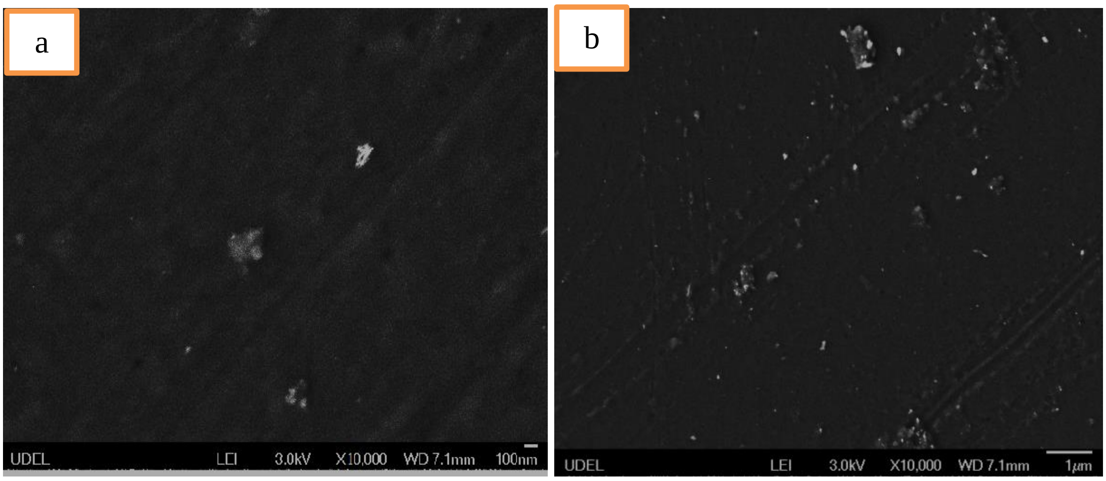

Fig. 3. FESEM images of different ratios of P3HT:PCBM:ZnO:TiO_2 active layer.

Fig. 3(a)-3(b) show the field emission scanning electron microscope (FESEM) images of the active layer of D and E. Fig. 3a displays few small and large clusters of TiO_2 and ZnO were found on the surface of the active layer. In binary film E complete agglomeration was observed, as shown in Figure 3b. Due to complete agglomeration without PCBM in the active layer, it appears that PCBM also acts as surfactant for ZnO:TiO_2. This suggests it necessary to use an active layer of PCBM and ZnO:TiO_2 to achieve high performing devices.

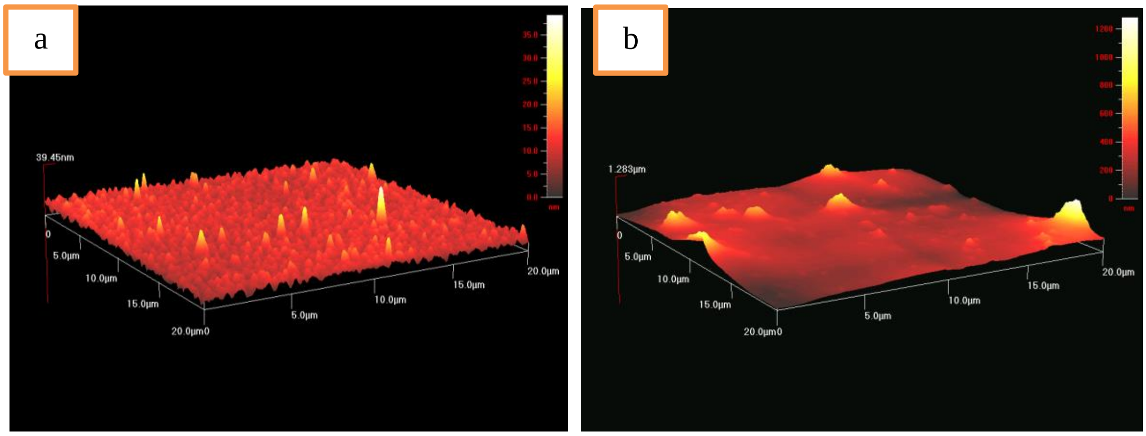

Fig. 4 (a &b) : AFM images of A and D active layers

The Fig. 4(a)-4(b) display images of A and D active layers obtained using atomic force microscope (AFM). Figure 4a represents the surface is rough with few needle type feature and a RMS roughness value of 5.7 nm. Fig. 4b shows the formation of small and large chunks of ZnO:TiO_2 on the surface of P3HT and PCBM with RMS roughness of 26.4 nm. This roughness increased with increasing amount of ZnO:TiO_2 in the blend of P3HT: PCBM film.

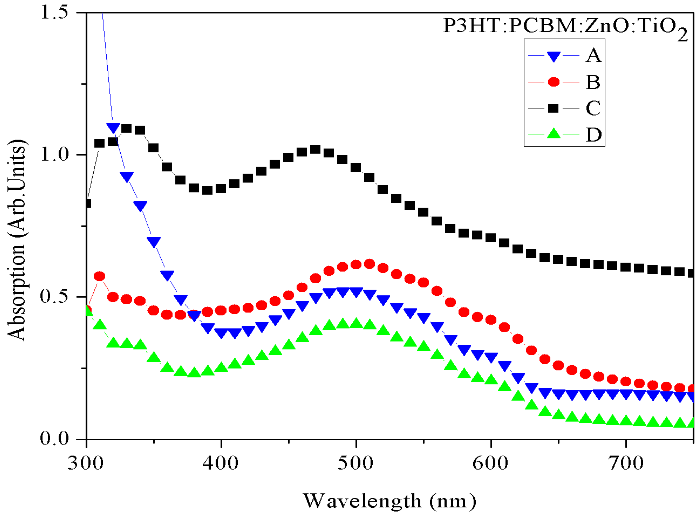

Fig. 5: Optical graphs of different ratios of P3HT:PCBM:ZnO:TiO$_2$ based devices.

The UV- Vis absorption spectra of various ratios of P3HT:PCBM:TiO$_2$:ZnO active layers prepared at 150^{0}C for 15 minutes is shown in Figure 5. In active layer A, the absorption of PCBM is dominant below 400 nm and absorption caused by P3HT is visible between 400-640 nm. As PCBM concentration reduces in the active layer, the absorption peak of P3HT at 500 nm increases and broadens. This trend depends on PCBM concentration and thermal annealing of the active layer [31]. Absorption increased with increasing amount of ZnO:TiO$_2$ in the blend of P3HT:PCBM and introduced red and blue shift in the absorption spectra. As described earlier, roughness increased in the presence of nanoparticles in the active layer. The surface with high roughness might scatter more light and leads to slightly increased absorption with nanoparticles conjugated active layer [25].

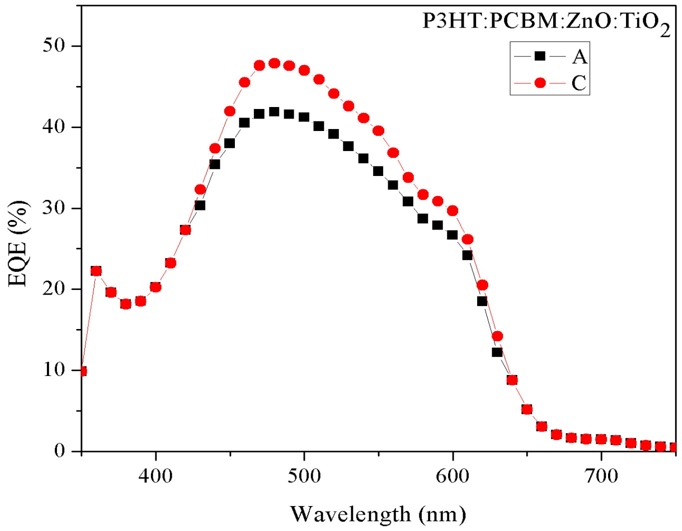

Fig. 6: EQE curves of different ratios of P3HT:PCBM:ZnO:TiO$_2$ blend devices.

The external quantum efficiency (EQE) curves of A and C devices are shown in Fig. 6. The figure shows the improved EQE with incorporation of ZnO and TiO$_2$ nanoparticles in the active layer of the devices. The enhancement in EQE was attributed to decrease in recombination current and to increased absorption in the active layer with incorporation of both nanoparticles [32].

4. Conclusions

Effects of incorporation of ZnO and TiO_2 nanoparticles in the active layer of P3HT:PCBM BHJ solar cells was studied. The mixing shows an increase in the efficiency of the devices from 1.13±0.04 % to 2.22±0.03 %. The efficiency improved most probably due to decrease in Rs of the devices. The Voc, Jsc, FF and EQE of the devices increases with increasing amount of both nanoparticles in the blend of active layer of P3HT:PCBM. The addition of both nanoparticles enhanced the absorption and introduce blue shift with optimum amount of ZnO:TiO_2 in the blend of the active layer. The ZnO and TiO_2 nanoparticles agglomerated with increasing amount of nanoparticles in the active layer and increased the surface roughness. The both nanoparticles formed large aggregates in the absence of PCBM in the active layer. This recommends that the PCBM also acted as a surfactant material in the photoactive layer of the devices.

Acknowledgement

The work is jointly supported by National Academy of Science (NAS), USA and Higher Education Commission (HEC) Pakistan.

References

[1] Y. Zhou, C. Fuentes-Hernandez, J. Shim, J. Meyer, A.J. Giordano, H. Li, Science **336**, 327 (2012).
[2] B. Kippelen, J.-L. Brédas, Organic photovoltaics, Energy & Envir. Science., **2**, 251 (2009).
[3] Z. He, C. Zhong, S. Su, M. Xu, H. Wu, Y. Cao, Nature Photonics. **6**, 593 (2012).
[4] C.J. Brabec, S. Gowrisanker, J.J.M. Halls, D. Laird, S. Jia, S.P. Williams, Advanced Materials **22**, 3839 (2010).
[5] A. Keawprajak, P. Piyakulawat, A. Klamchuen, P. Iamraksa, U. Asawapirom, Solar Energy Materials and Solar Cells., **94**, 531 (2010)
[6] F. Peng, J. Wu, Q. Li, Y. Wang, G. Yue, Y. Xiao, Electrochimica Acta., **56**, 5184 (2011).
[7] S.-S. Kim, J. Jo, C. Chun, J.-C. Hong, D.-Y. Kim, Journal of Photochemistry and Photobiology A: Chemistry. **188**, 364 (2007).
[8] D. Deng, M. Shi, F. Chen, L. Chen, X. Jiang, H. Chen, Solar Energy., **84**, 771 (2010).
[9] M.C. Arenas, N. Mendoza, H. Cortina, M.E. Nicho, H. Hu, **94**, 29 (2010).
[10] M. Al-Ibrahim, Flexible, Solar Energy Materials and Solar Cells., **85**, 13 (2004).
[11] B. Reeja-Jayan, A. Manthiram, Solar Energy Materials and Solar Cells., **94**, 907 (2010).
[12] T.-L. Wang, C.-H. Yang, Y.-T. Shieh, A.-C. Yeh, L.-W. Juan, H.C. ZengEuropean Polymer Journal. **46**, 634 (2010).
[13] J.-S. Huang, C.-Y. Chou, M.-Y. Liu, K.-H. Tsai, W.-H. Lin, C.-F. Lin, Organic Electronics. **10**, 1060 (2009).
[14] J.H. Lee, J.H. Park, J.S. Kim, D.Y. Lee, K. Cho, Organic Electronics. **10**, 416 (2009).
[15] W.-J. Yoon, K.-Y. Jung, J. Liu, T. Duraisamy, R. Revur, F.L. Teixeira, et alSolar Energy Materials and Solar Cells. **94**, 128 (2010).
[16] W.-H. Baek, T.-S. Yoon, H.H. Lee, Y.-S. Kim, Organic Electronics., **11**, 933 (2010).
[17] W.-L. Lu, Y.-S. Fu, B.-H. Tseng, Journal of Physics and Chemistry of Solids. **69**, 637 (2008)
[18] S H. Hu,.C. Kung, L.-M. Yang, M.E. Nicho, R.M. Penner, Solar Energy Materials and Solar Cells., **93**, 51 (2009).
[19] G. Kalita, M. Masahiro, W. Koichi, M. Umeno, Solid-State Electronics. **54**, 447 (2010).
[20] M. Wang, X. Wang, Solar Energy Materials and Solar Cells., **92**, 357 (2008)
[21] L.H. Slooff, M.M. Wienk, J.M. Kroon, Thin Solid Films., **451-452**, 634 (2004).
[22] M. Wang, X. Wang, Solar Energy Materials and Solar Cells., **91**, 1782 (2007).
[23] B.R. Saunders, Journal of Colloid and Interface Science., **3691**–15. 2012
[24] N.R. Mathews, E.R. Morales, M.A. Cortés-Jacome, J.A. Toledo Antonio, Solar Energy. **831499**, 1508 (2009).

[25] S.H. Oh, S.J. Heo, J.S. Yang, H.J. Kim, ACS Applied Materials & Interfaces. **5**, 11530 (2013).
[26] J.-F. Lin, G.-Y. Tu, C.-C. Ho, C.-Y. Chang, W.-C. Yen, S.-H. Hsu, ACS Applied Materials & Interfaces., **5**, 1009 (2013).
[27] B.R. Saunders, M.L. Turner, Advances in Colloid and Interface Science., **138**, 1 (2008).
[28] N. Zhao, T.P. Osedach, L.-Y. Chang, S.M. Geyer, D. Wanger, M.T. Binda, et al., ACS Nano., **4**, 3743 (2010).
[29] E.L. Lim, C.C. Yap, M. Yahaya, M.M. Salleh,Journal of Physics: Conference Series. **431**,12017 (2013).
[30] H. Fu, M. Choi, W. Luan, Y.-S. Kim, S.-T. Tu, Solid-State Electronics., **69**, 50 (2012).
[31] Y.-Y. Yu, W.-C. Chien, Y.-H. Ko, Y.-C. Chan, S.-C. Liao, Current Applied Physics. **12**, S7 (2012).
[32] G. Li, V. Shrotriya, Y. Yao, J. Huang, Y. Yang, J. of Mat. Chem. **17**, 3126 (2007).